



Science Arts & Métiers (SAM)

is an open access repository that collects the work of Arts et Métiers Institute of Technology researchers and makes it freely available over the web where possible.

This is an author-deposited version published in: <https://sam.ensam.eu>
Handle ID: <http://hdl.handle.net/10985/8592>

To cite this version :

Guillaume MARTIN, Etienne BALMES, Thierry CHANCELIER - Improved Modal Assurance Criterion using a quantification of identification errors per mode/sensor - In: International Conference on Noise and Vibration Engineering, Belgium, 2014-09-15 - Proceedings ISMA - 2014

Any correspondence concerning this service should be sent to the repository

Administrator : scienceouverte@ensam.eu



Improved Modal Assurance Criterion using a quantification of identification errors per mode/sensor

Guillaume Martin^{1,2}, Etienne Balmes^{1,2}, Thierry Chancelier³

¹Arts et Metiers ParisTech

151 Boulevard de l'Hôpital, 75013, Paris, France

²SDTools

44 rue Vergniaud, 75013, Paris, France

e-mail: balmes@sdtools.com

³Chassis Brakes International

126 rue de Stalingrad, 93700, Drancy, France

Abstract

Scanning laser vibrometer measurements generate detailed maps of modal characteristics in normal or 3D directions. Since many points are measured, individual validation of cannot be performed manually in a reasonable time frame and a notable fraction of measurements is expected to be fairly noisy. The key new notion of the paper is a quantification of identification error and level of contribution for each mode and each sensor based on the comparison of measured and synthesized transfers around each resonance. These criteria are shown to allow efficient analysis of the validity of large measurement sets to provide an automated procedure to select sensors that should be kept for each mode. This quantification, being performed before correlation, provides a priori estimates of sources of poor correlation associated with the identification process. It thus becomes possible to provide improved Modal Assurance Criterion estimations where, for each modeshape, sensors known to be incorrectly identified can be discarded. The 3D vibrometer scan of a brake component is used to illustrate the proposed strategies.

1 Introduction

Laser vibrometer scans are routinely used by Chassis Brakes international in the model validation process where brake components and assemblies are tested and correlated with FEM models. Such measurements generate detailed maps of modal characteristics in normal or 3D directions. Compared to classical modal analyzes with accelerometers, many more points are measured. As a result individual validation of measurements cannot be performed manually in a reasonable time frame and a notable fraction of measurements is expected to be fairly noisy.

Taking the classical Modal Assurance Criterion (MAC) [13], the need to diagnose sensors contributing to poor correlation was identified very early and led to the CoMAC [1], eCoMAC criteria [2] or MACCo [3, 4] criteria. All these approaches assume the identification to be correct and seek to identify sensors that contribute to poor correlation between test and model results. They can thus be qualified as *a posteriori* estimates of errors associated either to identification or modeling.

The key notion introduced in section 2 is an *a priori* quantification of identification error for each mode and each sensor based on the comparison of measured and synthesized transfers around each modal resonance. This criterion does not imply the need to use stochastic methods to estimate uncertainty bounds on modal

parameters [5, 6] and is thus more easily used. A related criterion of contribution is also introduced to ease the distinction of sensors that may be important despite significant error levels. Taking identification results obtained using the pole tuning strategy [7] of the Structural Dynamics Toolbox [4] for MATLAB, these criteria are shown to allow proper quantification of sensor sets with good identification.

This quantification, being performed before correlation, provides a priori estimates of sources of poor correlation associated with the identification process. It thus becomes possible to provide improved MAC estimations, where, for each modeshape, sensors to known to be incorrectly identified can be discarded. Illustrations of this process are given in section 3.

Throughout this paper, the proposed methods will be applied to test shown in Figure 1. The measurement is done on a press-formed plate part of a drum brake using a 3D scanning laser vibrometer. To be as close as possible to the free-free conditions used by the finite element model, the plate is suspended with a fishing line and is impacted with an automated hammer. Multiple acquisitions are made for 322 points generating 966 transfer functions.



Figure 1: Test configuration with automated impact and 3D scanning vibrometer measurement

2 Identification error

While many identification procedures exist [8, 9], the identification errors are rarely quantified. When actually addressed [6, 5], the strategy is generally based on statistics and thus are not applicable to cases where the main error is a form of bias. After showing the classical estimation of modes and residual terms based on known poles that is commonly used in most modal analysis packages, one shows that the resulting superposition can be used to introduce identification errors and contributions per mode and sensor and illustrates the possible resulting analyzes.

2.1 Identification in the pole-residue form

A critical aspect of identification algorithms is the form of the considered parametric model. For applications in structural dynamics, the reference model is the **rational fraction** decomposition using first order fractions (also called **pole/residue** model)

$$[H_{id}(s)] = \sum_{j \in \text{identified}} \left(\frac{[R_j]}{s - \lambda_j} + \frac{[\bar{R}_j]}{s - \bar{\lambda}_j} \right) + [E(s)] + [F(s)] \quad (1)$$

where the residue matrix $[R_j] = \{c\psi_j\} \{\psi_j^T b\}$ is given by the product of a column observability $\{c\psi_j\}$ and row controllability $\{\psi_j^T b\}$ (see [7] for details). In the literature [8], the residue is often written $[A_j] = \{\psi_j\} \{L_j\}$ where modeshape and observability are thought to be the same and the controllability is called modal participation factor L_j . The notation used here, while less common, emphasizes the duality between inputs and outputs.

Residual terms $[E(s)]$ and $[F(s)]$ are characteristic of the transfer being considered (high frequency modes contribute a constant for displacement measurements and a $[E] s^2$ contribution for acceleration, low frequency modes contribute a $\frac{[F]}{s^2}$ for displacement measurements and a constant contribution for acceleration). For known poles (estimated by any appropriate method and [7] in the present case), model (1) depends linearly on residues and residual terms $[R_j(\lambda_j), E, F]$. One can thus estimate those terms by solving the linear least squares problem associated with the frequency domain output error

$$[R_j(\lambda_j), E, F] = \arg \min \left| [\alpha(s)]_{test} - \sum_{j=[1, NM]} \left(\frac{[R_j]}{s - \lambda_j} + \frac{[\bar{R}_j]}{s - \bar{\lambda}_j} \right) + [E(s)] + [F(s)] \right|^2 \quad (2)$$

The approach is fairly standard and quite efficient even for problem with many channels. It is however

- quite sensitive to errors on the position of poles [7]
- does not account for constraints on multiplicity (MIMO tests), reciprocity or second order representation [10]

2.2 Identification error and contribution per mode and sensor

Superposition of identified and measured transfers is very classically used as a qualitative indication of identification quality. The important contribution of the paper is to show how it can be used quantitatively in a test/analysis correlation process.

To look at each input/output pair and compare them individually, one rewrites equation (1) for each measurement channel c

$$H_{id,c}(s) = \sum_{j \in \text{identified}} (H_{idj,c}(s)) + E_c(s) + F_c(s) \quad (3)$$

The contribution of a mode is well known to be maximal around its resonance. It is thus classical to focus identification to the half power bandwidth given by $[\omega_j(1 - \zeta_j) \ \omega_j(1 + \zeta_j)]$ with ω_j the resonance frequency and ζ_j the modal damping. One thus defines an identification **error** for mode j and input/output c pair as

$$e_{j,c} = \frac{\int_{\omega_j(1-\zeta_j)}^{\omega_j(1+\zeta_j)} |H_{Test,c}(s) - H_{id,c}(s)|^2}{\int_{\omega_j(1-\zeta_j)}^{\omega_j(1+\zeta_j)} |H_{id,c}(s)|^2} \quad (4)$$

This error can be viewed as a numerical evaluation of the quality of the historical "circle fit" method.

When using the proposed identification error, one finds cases where certain modes presenting high error values are nevertheless well visible in the transfer function. It was thus found important to introduce a quantification of "visibility" of a given mode to the transfer, called **contribution**, and defined by

$$C_{j,c} = \max \left(0, 1 - \frac{\int_{\omega_j(1-\zeta_j)}^{\omega_j(1+\zeta_j)} |H_{Test,c} - H_{idj,c}|^2}{\int_{\omega_j(1-\zeta_j)}^{\omega_j(1+\zeta_j)} |H_{Test,c}|^2} \right). \quad (5)$$

The choice of H_{Test} rather than H_{Id} in the contribution is subject to discussion. Using H_{Id} was found to generate false positives where the estimated contribution is high for very noisy signals where one can actually not expect to identify anything.

Figure 2 shows transfer functions for representative sensors. The mode of interest is the last of the band (near 2473 Hz shown as a vertical dotted line). The simple cases are those with high contribution and low error, illustrated in Figure 2b. Figure 2a correspond to the case where the mode is not noisy but contribute very little to the transfer. Such cases need to be looked at in more detail since the estimated modeshape may easily be biased. Figure 2d corresponds to another case that needs to be analyzed since the significant noise generates high error but the contribution is sufficient to allow fairly good identification. The problematic sensors are those with high error and low contribution 2c and such sensors should be ignored without hesitation.

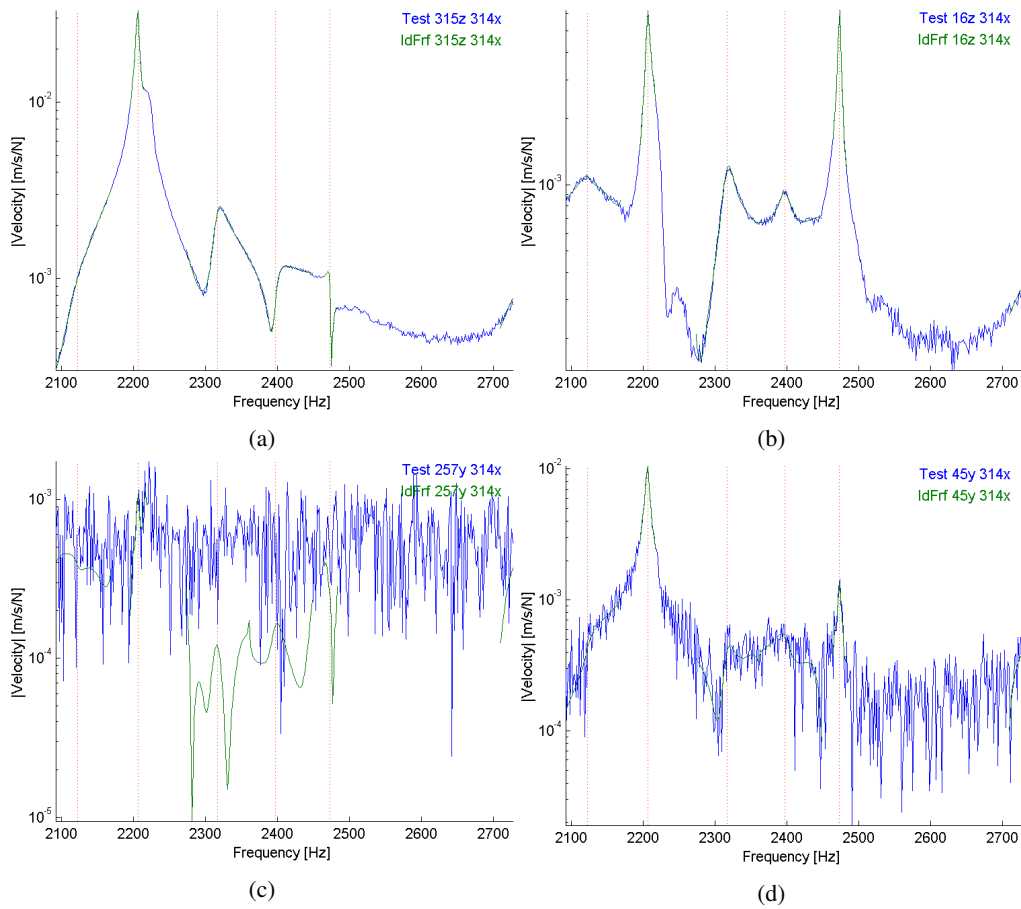


Figure 2: Error And Contribution visualisation on FRF : (a) Low Error Low Contribution, (b) Low Error High Contribution, (c) High Error Low Contribution, (d) High Error High Contribution.

2.3 Sensor set selection

Since the error and contributions are given for each sensor, one can define a valid sensor set of each mode. The procedures to generate these sets are illustrated below by focusing on two mode shapes presented in Figure 3. Mode 4 is a global bending mode, while mode 14 is mostly localized around the center hole. The error and contribution for these two modes are shown in Figure 4.

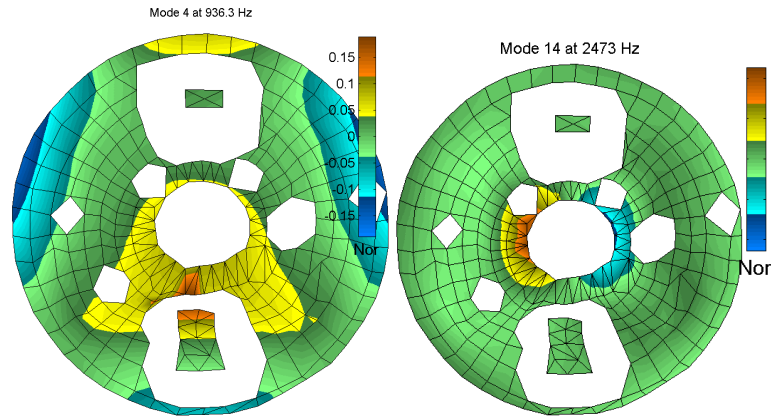


Figure 3: Visualization of two modeshapes in the normal direction. Modes 4 left and 14 right.

The global nature of mode 4 is highlighted by the fact that many more sensors have a high contribution (red curve close to 0.5). As normally expected, high errors are only found for sensors where the mode has a low contribution. The RMS level in the associated area (shown as a green) is small and thus more likely to be noisy and showing errors.

For mode 14, error levels are significantly higher but many are associated with low contributions and the ability to perform proper identification can thus be questioned. The contribution criterion shows low levels, so the choice to ignore these sensors is confirmed.

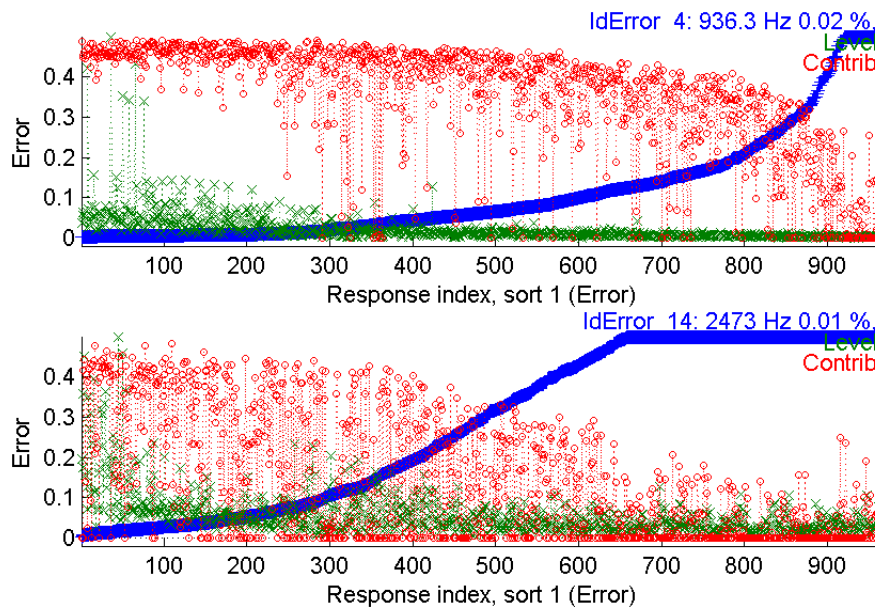


Figure 4: Error (blue), contribution (red) and RMS level (green) for mode 4 (top) and 14 (bottom)

The viewing by sorted sensors in figure 4, loses the important information of where these sensors are located. It is thus interesting to reformat this information as maps in the x , y and z directions shown in Figure 5. The error (on top) is very important for all in-plane sensors. This could be expected here because it is well known that with laser vibrometer measurement, noise is higher in the plane orthogonal to the measurement direction. This is increased here by the fact that the considered mode has very low in plane displacement. The contribution plot, confirms that very few sensors respond in plane, but also indicates that many out-of-plane sensors have very low error despite low contributions, thus confirming the validity of the characterization as a local mode.

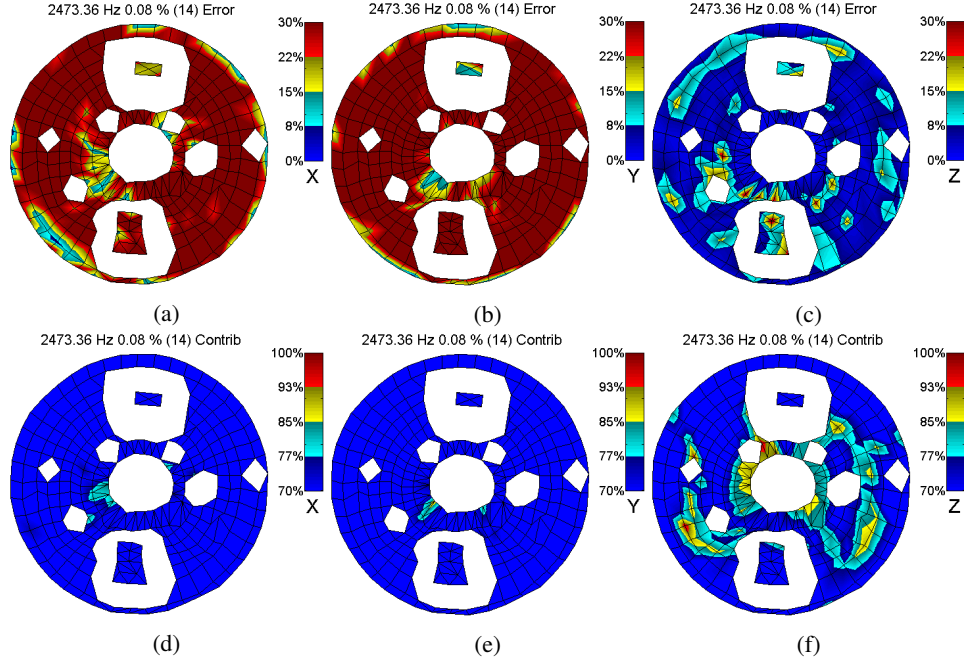


Figure 5: Top : error in the x , y and z direction for mode 14. Bottom: contribution in the same directions.

3 Improving the Modal Assurance Criterion using identification error

Given the methodology to associate a quality for each sensor and each mode, it becomes obvious that this information should be used for correlation. One first reminds that topology correlation often is a major source of error, then summarizes correlation criteria and associated sensor classification strategies from the literature and finally illustrates how improved correlation can be obtained.

3.1 Topology correlation

When performing test/analysis correlation, the basic inputs are the identification result discussed in section 2, the finite element simulation and the topology correlation which extracts the FEM data at sensors, so that a direct comparison of responses is possible. While identification error is the focus of this paper, it is useful to insist on the fact that topology correlation can be a significant source of errors [11].

Since tests are known at sensor/actuator pairs and FEM models at Degree of Freedom (DOF), there is a mismatch in the spatial dimensions. The extraction of FEM responses at sensors can be described by an observation equation

$$\{y\}_{NS} = [c]_{NS \times N} \{q\}_N \quad (6)$$

where outputs $\{y\}_{NS}$ are linearly related to DOF $\{q\}$. The building of the observation matrix $[c]$ is often referred to as topology correlation. Nearest-node and rigid link approximation are the simplest approaches. More accurate strategies use orthogonal projection of the sensor positions to the surface of matching elements and underlying FEM shape functions to properly estimate the motion at sensors. Steps of topology correlation typically involve adjustment of the test-wire frame reference frame to match that of the FEM and position matching.

An Iterative Closest Point (ICP) algorithm has been implemented here to optimize the positioning of the test-wireframe on the FEM model. As the matching is performed using an orthogonal projection on the surface, the cost function to be minimized is the norm of the distance for each sensor to the FEM. Considering the initial position, found with three corresponding points given manually, is close to the optimum, the cost

function has been linearized to increase computation speed, in a procedure similar to that proposed in [12]. Figure 6 illustrates the topology correlation result of the considered application.

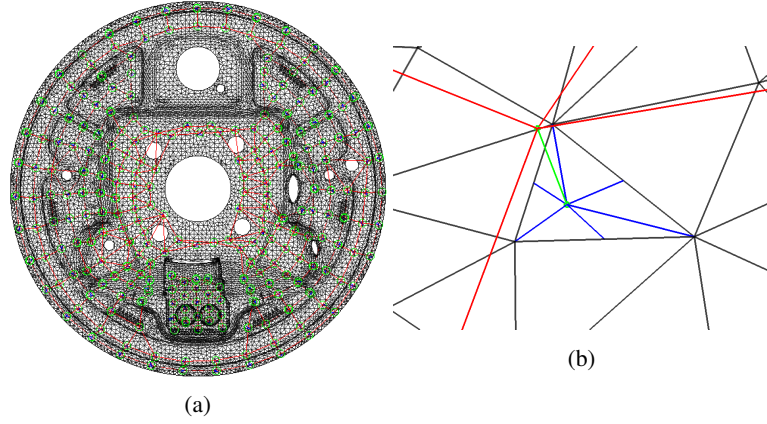


Figure 6: Sensor matching on FEM : (a) Global position, (b) Projection (green) and Observation (blue),

3.2 Classical shape correlation criteria (MAC, COMAC)

Having test and FEM shapes at sensor $[c] \{\phi\}$ and identified modeshapes $\{c\phi_{id}\}$ (where obviously the observation is physical), the MAC [13] computes the correlation coefficient given by

$$MAC_{jk} = \frac{|\{c\phi_{idj}\}^H [c] \{\phi_k\}|^2}{|\{c\phi_{idj}\}^H \{c\phi_{idj}\}| |\{\phi_k\}^H [c]^H [c] \{\phi_k\}|} \quad (7)$$

and thus provides a normalization independent quantification of whether modeshapes are linearly related [13]. A MAC value above 0.9 is typically considered good while a value below 0.7 normally corresponds to poor correlation.

The need for localization of poor correlation was identified very early and led to different approaches.

The CoMAC [1] uses the same orthogonality criterion as the MAC, but instead of comparing data of all sensors at each mode shape j , it compares data of all mode shapes at sensor c

$$COMAC_c = 1 - \frac{\left\{ \sum_{j=1}^{NM} |c\phi_{j,c}^A c\phi_{j,c}^B| \right\}^2}{\sum_{j=1}^{NM} |c\phi_{j,c}^A|^2 \sum_{j=1}^{NM} |c\phi_{j,c}^B|^2} \quad (8)$$

where the 1– definition is used here to have good correlation for high values of COMAC. This definition of COMAC assumes that modes are similarly scaled. As this is sometimes difficult to ensure, a **scaled** COMAC is computed with shapes in set B scaled using the Modal Scale Factor (MSF)

$$\{\widehat{c\phi_{jB}}\} = \{c\phi_{jB}\} MSF_j = \{c\phi_{jB}\} \frac{\{c\phi_{jB}\}^T \{c\phi_{jA}\}}{\{c\phi_{jB}\}^T \{c\phi_{jB}\}} \quad (9)$$

which sets the scaling of vectors in set B to minimize the quadratic norm of the difference between $\{c\phi_{jA}\}$ and $\{\widehat{c\phi_{jB}}\}$.

While the CoMAC theory is quite old, the number of papers reporting its use is fairly limited. A reason for this limitation is probably that it needs a number of identified modes to be relevant in pointing sensors that globally contribute to a poor correlation. The second limitation is rightly contained in the global nature of this criterion: as shown in 2.3, sensors may not contribute for a lot of modes but be very relevant for some others (especially local ones), and such a criterion could tend to remove them.

The **enhanced** COMAC (eCOMAC), introduced in [2], uses the mean of step between modal amplitude for each sensor on all modes, despite of the orthogonality criterion. It is given by

$$eCOMAC_l = \frac{\sum_j^{NM} \left\| \{c_l \widetilde{\phi}_{jA}\} - \{c_l \widetilde{\phi}_{jB}\} \right\|}{2NM} \quad (10)$$

where the comparison is done using modeshapes that are vector normalized to 1 with

$$\{c_l \widetilde{\phi}_{jA}\} = \{c_l \phi_{jA}\} / \|c_l \phi_{jA}\|$$

As for the original COMAC, it needs enough identified modes and works on a global removal for all modes. A last criterion is known by different names : the MAC Variation Technique [3] or the MAC coordinate criterion (MACCo) [4]. This iterative algorithm successively removes sensors that contributed to low MAC values. The structure of the algorithm is detailed in Figure 8. Comparatively to COMAC variants, it is possible to compute different sets of removed sensors. Using the mean MAC for paired modes is typically useful to detect poor sensors (global removal of sensors), while removal for a specific mode is used to understand the source of poor correlation.

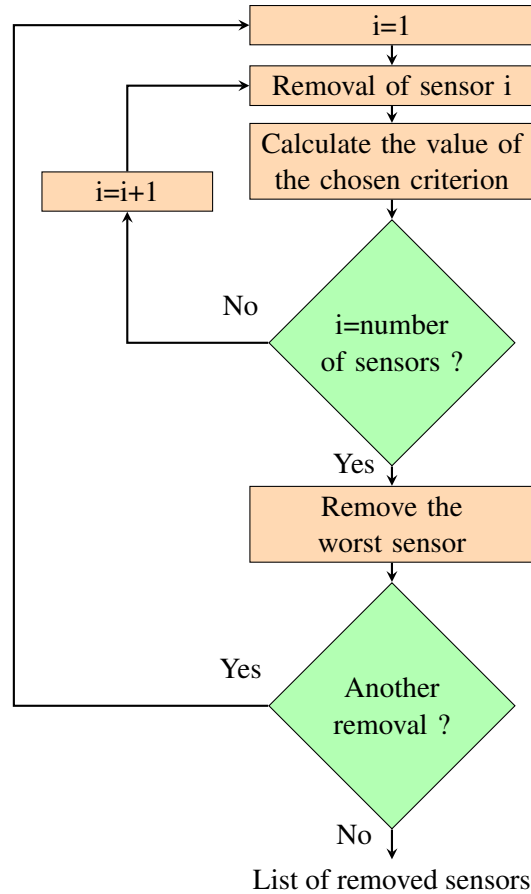


Figure 7: MACCo Algorithm

The main drawback of the MACCo is that it cannot make the difference between a sensor removed because of a wrong identification and a sensor which should be kept because it really shows a difference of behavior between the finite element model and the test. This motivates the proposed MAC-Error where the identification error is used to sort sensors.

3.3 Improved MAC

The FEM model of the example chosen for this paper actually ignored significant features present in the test, so that test/analysis correlation was only relevant for a few modes. Mode 14 (see Figure 3) was of particular interest.

Figure 8 shows the MACCo result that only seeks to remove sensors that contribute to poor correlation. This figure indicates that removing only 10% of sensors improves the correlation tremendously to 0.85. The bottom plot shows that these sensors are removed for in-plane directions, which seems relevant. But the question remains of whether useful information was removed.

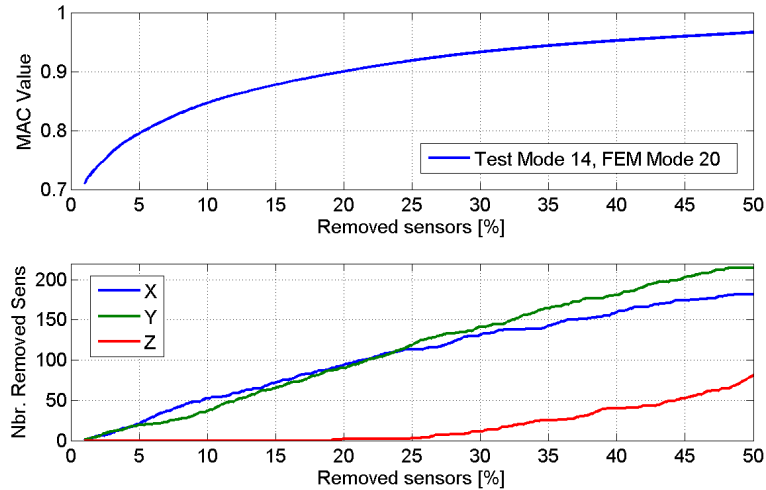


Figure 8: MAC evolution

The MAC-error strategy one can use the error criterion to eliminate the least relevant sensors. Figure 9 top shows the evolution of the computed MAC, when sensors with too high an error are removed. Experimentally, 30 % error is typically corresponds to transfers that are so noisy that any identification is irrelevant. Figure 9 bottom shows that about 50% of the sensors have been removed for this threshold but that they essentially correspond to in-plane motion and is known to be noisier in this configuration. This is quite consistent with the orientation maps shown in Figure 5.

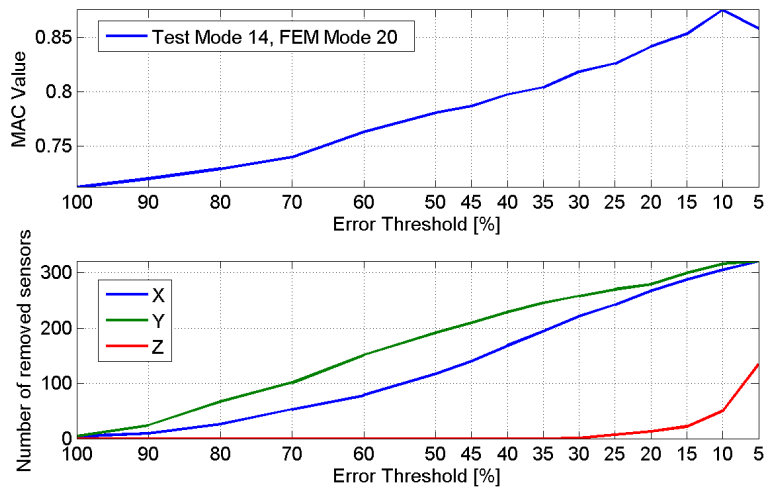


Figure 9: MAC evolution with error threshold

With the removal, one see that the MAC is improved from 70% to near 80%, thus noticeably changing the perspective on the correlation of this mode. But this value is lower than that found with the MACCo thus showing that significant differences remain.

4 Conclusion

The paper proposed a strategy to analyze the experimental validity of each modeshape component at each sensor. This strategy is well suited for 3D scanning vibrometer tests with many measurements and was shown to possibly notably change the correlation computed for some modes.

This initial work opens many questions. On the identification side, results could be improved by optimizing each pole with only a selection sensors. Sensors with a high level of error, and possibly with low contribution, have been found to introduce bias in the identification. Selecting only relevant transfers to estimate the pole should reduce this bias, while (2) could still be considered for shape estimation. In the practice of tests, the criteria provided can also be used as diagnostic tools to improve the quality of tests, by easily highlighting areas with high contributions and significant error levels.

On the correlation side, the example chosen is not ideal because of an incomplete FEM model. Regular use on other test cases will bring understanding of how the proposed strategy of defining sensor sets associated with each mode can be used to show which parts of problems in correlation come from test, seen as identification error, and which come from modeling, seen as residual differences or localized with the MACCo.

References

- [1] N. Lieven and D. Ewins, "Spatial correlation of modeshapes, the coordinate modal assurance criterion (comac)," *International Modal Analysis Conference*, 1988.
- [2] D. Hunt, "Application of an enhanced coordinate modal assurance criterion," *International Modal Analysis Conference*, pp. 66–71, 1992.
- [3] M. Brughmans, J. Leuridan, and K. Blauwkamp, "The application of fem-ema correlation and validation techniques on a body in white," *IMAC*, pp. 646–654, 1993.
- [4] *Structural Dynamics Toolbox (for use with MATLAB)*. SDTools, Paris, France, www.sdtools.com, Sep 1995-2014.
- [5] R. Pintelon, P. Guillaume, and J. Schoukens, "Uncertainty calculation in (operational) modal analysis," *Mechanical Systems and Signal Processing*, vol. 21, pp. 2359–2373, 2007.
- [6] E. Reynders, R. Pintelon, and G. D. Roeck, "Uncertainty bounds on modal parameters obtained from stochastic subspace identification," *Mechanical Systems and Signal Processing*, vol. 22, pp. 948–969, 2008.
- [7] E. Balmes, "Frequency domain identification of structural dynamics using the pole/residue parametrization," *International Modal Analysis Conference*, pp. 540–546, 1996.
- [8] W. Heylen, S. Lammens, and P. Sas, *Modal Analysis Theory and Testing*. KUL Press, Leuven, Belgium, 1997.
- [9] D. Ewins, *Modal Testing: Theory and Practice*. John Wiley and Sons, Inc., New York, NY, 1984.
- [10] E. Balmes, "New results on the identification of normal modes from experimental complex modes," *Mechanical Systems and Signal Processing*, vol. 11, no. 2, pp. 229–243, 1997.
- [11] T. França de Paula, G. Rejdych, T. Chancelier, G. Vermot des Roches, and B. E., "On the influence of geometry updating on modal correlation of brake components.," in *Proceedings VCB*, 2012.
- [12] K.-L. Low, "Linear least-squares optimization for point-to-plane icp surface registration," *Chapel Hill, University of North Carolina*, 2004.

- [13] R. Allemang, “The modal assurance criterion (mac): twenty years of use and abuse,” *International Modal Analysis Conference*, pp. 397–485, 2002.